

PAPER from 12th International Colloquium Fuels Conventional and Future Energy for Automobiles.  
25<sup>th</sup>-26<sup>th</sup> June 2019 Technische Akademie Esslingen in Stuttgart/Ostfildern.

Permission is given for storage of one copy in electronic means for reference purposes. Further reproduction of any material is prohibited without prior written consent of Innospec Inc.

©INNOSPEC INC 2019

All rights reserved.

# Detailed characterisation of diesel fuel filter deposits by ToF-SIMS and other analytical methods

Matteo Spanu  
University Of Nottingham, Nottingham, UK

Jim Barker, David Pinch and Jacqueline Reid  
Innospec, Ellesmere Port, UK

David Scurr, Colin Snape and William Meredith  
University Of Nottingham, Nottingham, UK

## Summary

Through time of flight secondary ion mass spectrometry (ToF-SIMS) of filters from the multi-pass filtration test, engine tests and field samples, a detailed compositional breakdown of inorganic and organic contaminants was obtained. Using principal component analysis, it was possible to account for 91% of the chemical variance in the first two self-defined principal components of the ions obtained in ToF-SIMS. The first principal component, which accounts for over 80% of the variance, is dominated by sodium, which was ubiquitous in all the samples analysed. The second principal component with contributions from aliphatic species accounted for a further 10% of the variance. In addition to the TOF-SIMS results, a combination of in-situ and invasive analytical techniques are being used. Scanning electron microscopy (SEM) used to compare the morphology of the filter deposits and correlate with the trends identified from ToF-SIMS found the presence of sodium soaps when organic films were present on the filter surface.

## 1. Introduction

The recent advancements in internal combustion engine designs, instigated by changing emission legislation, have required an increase in fuel filtration efficiency as well as the need for the use of ultra-low sulfur diesel (ULSD). The process used to remove sulfur species from diesel has been reported to also remove other polar compounds from fuel which contribute to its lubricity [1-3]. In parallel with the shift to fuel injection equipment (FIE) and the use of ULSD, there has been an increase in the reports of failure of FIE [4-6]. Previous studies have noted that the build-up of sodium salts in injectors is not solely the cause of internal diesel injector deposits (IDID) but a leading factor [5-10]. The sodium precursors originate upstream from the fuel pump whilst the acids are common in lubricity additives [5, 6]. The presence of low molecular weight polyisobutylene succinimides (PIBSI) has also been reported to be present in some IDIDs [6, 9, 11]. The cause of deposits on filters, in comparison with IDID, has been rarely discussed with only a few publications [5, 7, 12, 13].

It was through the use of Fourier-transform infrared spectroscopy (FTIR) and mass spectrum analysis that sodium carboxylates were found to be one of the main

causes of filter plugging [5-8, 10]. Engine tests have been developed to adulterated fuel with a variety of sodium sources to reproduce the formation of deposits found in the field [5-7].

The cause of poor filterability using reference fuel (RF-06) in engine tests with a variety of lubricity additives as well as field samples found similar sodium salts [5, 7]. A study by Csontos [12] establish that when a biodiesel blend was used in engine tests, a sediment containing metal carboxylates and degraded fuel compounds were present in plugged filters.

Although FTIR can provide a molecular fingerprint of a sample there is no information on the topography of the deposits. Scanning electron microscopy (SEM) and energy dispersive X-ray (EDX) have been used to characterise surface topography and to obtain elemental composition of IDIDs [7-9, 11, 14-16] and filter samples [7, 12, 13].

Time of flight – secondary ion mass spectrometry (ToF-SIMS) is a surface sensitive analytical method for spatially resolving chemical information. The benefit of ToF-SIMS is the comprehensive analysis in deducing the exact masses and confirming the chemical structures of the IDIDs to be sodium carboxylate

structures, as well as providing the spatial chemistries on the surface of a sample [9, 10, 17, 18]. No work to date has used ToF-SIMS to characterise the deposits on fuel filters.

The data sets generated from a ToF-SIMS analysis can be very large and to assist in the interpretation of the data sets, we have used principal component analysis (PCA), a multi variant analytical technique that can be used to highlight patterns in the data [17, 19]. Work by Barker et al. highlighted the ability to define the different constitutions of an IDID for different fuels [17].

## 2. Experimental methods

### 2.1 Samples and preparation

This limited study involves investigation of filters across a number of sources in order to inform on the nature of diesel fuel filter deposits. These encompass a wide variety of sources, blank filters, engine test filters, filter rig filters, and field failure filters.

In detail filter samples were taken from the field, engine tests and a modified multi-pass filtration rig, as well as control sample unused filters, and reference fuel only. (Table 1). Field samples were obtained from failed filters in North America, Europe and Asia. The engine test (a DW10B modified to C) used reference fuel (RF-06) and various combinations of added Deposit Control additive (DCA), sodium naphthenate (SN) and Dodecylsuccinic acid (DDSA). To mimic the deposits an adaptation of the multi-pass filtration method (ISO 19438) was adopted. The diesel used was the RF-06 standard with no added contaminants. Each sample was cut into 3 aliquots.

Table 1 Sample reference codes.

Filter type	Sample reference
Control	Sample 1
Control	Sample 2
Field USA	Sample 3
Field ASIA	Sample 4
Field EU	Sample 5
Engine test (SN+DDSA)	Sample 6
Engine test (DCA)	Sample 7
Engine test (Low level SN+DDSA and DCA)	Sample 8
Engine test (High level SN + DDSA and DCA)	Sample 9
Multi-pass test precursor	Sample 10
Multi-pass test	Sample 11

SEM and ToF-SIMS used for the analysis of the filters require the samples to be in a high vacuum. Therefore, all of the samples were vacuum oven dried at 140°C and 0.01 mbar prior to microscopy analysis to remove as much of the volatiles as possible.

### 2.2 Pyrolysis-GCMS

Samples were assessed on a 5000 series pyrolyzer (CDS analytical Inc.) directly connected to an Agilent 5977A series GC/MSD system. Pyrolysis – GCMS (Py-GCMS) on the samples before and after the vacuum drying, evaluated the hydrocarbon content and ensured that the samples were at a satisfactory level so as not to detrimentally impact the vacuum required in SEM and ToF-SIMS. The method was extended to a sequential method to test for the presence of long chained deposits on the filters which have higher thermal degradation properties than diesel.

Approximately 4 mg of sample was loaded into a quartz tube and held in place with quartz wool. To confirm the removal of diesel volatiles the pyroprobe was heated to 250°C at a rate of 10°C s<sup>-1</sup> then held for 1 minute. The interface was kept at 310°C and the transfer tube was at 280°C. Helium was used as the carrier gas at a rate of 1 ml min<sup>-1</sup> and split ratio of 75:1. The GC oven was heated from 40°C (2 minutes) to 300°C (5 minutes) at 6°C min<sup>-1</sup>.

The sequential method had the same GC, interface and transfer line parameters as the previous method. The pyroprobe, however, was incrementally increased to a final temperature of 250°C, 300°C, 350°C and 400°C at 10°C s<sup>-1</sup>.

### 2.3 SEM

A FEI Quanta 650 ESEM (environmental SEM) equipped with an Oxford Instruments energy dispersive x-ray (EDX) detection system was used. A low vacuum setting was chosen with a pressure between 60-650 Pa, an electron beam strength of 10-15kV and a spot size of 4 to obtain images of all the samples.

### 2.4 ToF-SIMS

The mass spectra of the filter deposits were obtained using a ToF-SIMS IV instrument (ION TOF GmbH). The primary ion beam used was a 25 keV Bi<sub>3</sub><sup>+</sup> ion gun to analyse the sample surface. The flood gun was on and a raster 500×500µm area of the surface of each sample was analysed with a lateral resolution of 256×256 pixels. The MS data of each sub-sample is then normalised with respect to the total ion intensity allowing comparison between the samples.

### 2.5 PCA

Owing to the large data sets are produced when analysing all of the samples using ToF-SIMS, a comparison between a number of samples becomes difficult. Hence PCA was used to initially deconvolute the ToF-SIMS data. PCA works on the theory that principal components (PC) are produced from observations to show possibly correlated variables. The

transformation results in the first PC accounting for the largest possible variance in the data, each proceeding PC has the largest possible variance under the constraint that it is orthogonal to the preceding components. PCA was computed in MATLAB using the 'pca' function with the variables mean centred and calculated in the singular value decomposition (SVD) of X mode.

### 3. Results and discussion

#### 3.1 Py – GCMS FIELD SAMPLES

The total ion chromatogram (TIC) from pyrolysis at 250°C held for 1 minute of the field filter sample 3 (USA) confirmed the presence of hydrocarbons for a typical diesel with n-alkanes dominating (Fig. 1).

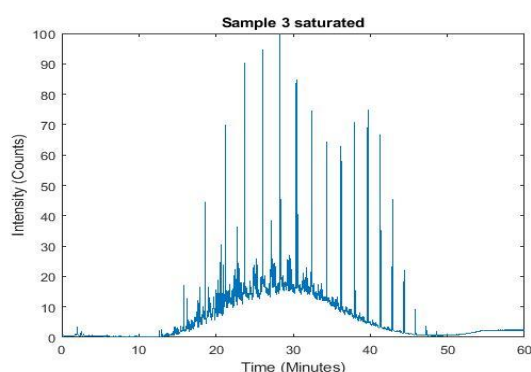


Fig. 1 TIC of field sample 3 from pyrolysis before vacuum drying.

Py-GCMS of the filter sample after vacuum drying confirmed the removal of diesel from the filter (Fig. 2) with the exception of extremely high boiling material (n-C<sub>25</sub> and n-C<sub>26</sub> dominating). On the basis of the comparative peak size from the TIC it was possible to deduce that 95% of the hydrocarbons were removed during vacuum drying.

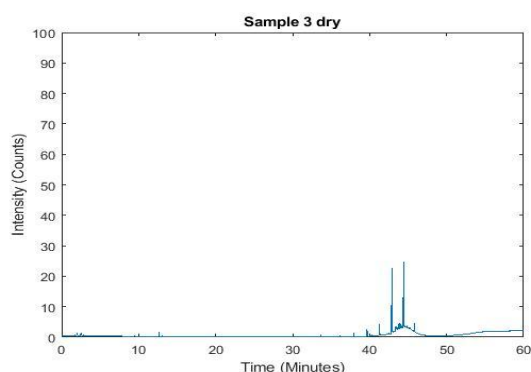


Fig. 2 TIC of field sample 3 from pyrolysis after vacuum drying.

Once this initial method was complete, pyrolysis was used to check the presence of deposits after the hydrocarbons from the fuel had been removed. The

sequential method used to heat field 4 mg of non-vacuum dried sample 4 to 250, 300, 350 and 400°C, collecting the exhaust gas in the GCMS between each temperature. At 250°C the TIC was dominated by the presence of hydrocarbons from the diesel, similar to that seen in sample 3 (Fig. 1). At 300°C there was the onset of oxygenated species from the cellulose (Fig. 3). This is a result of filter breakdown.

Analysis of filter sample 4 (ASIA) showed the following.

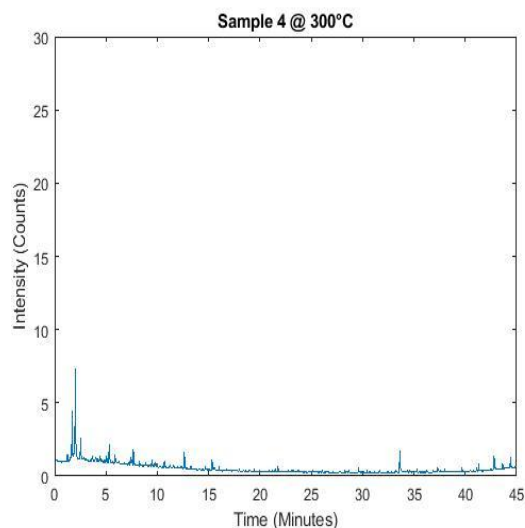


Fig. 3 TIC of field sample 4 from pyrolysis at 300C.

At 350°C, before 30 minutes, common peaks seen in pyrograms of polysaccharides (cellulose) [20] were characterised by their mass spectra. Attributable to the constituents of the filter medium. At 33:36 (min:sec) a peak that is likely hexadecanoic acid was observed (Fig. 4). This indicates the presence of acids in the sample, interpreted to be derived from a carboxylate soap.

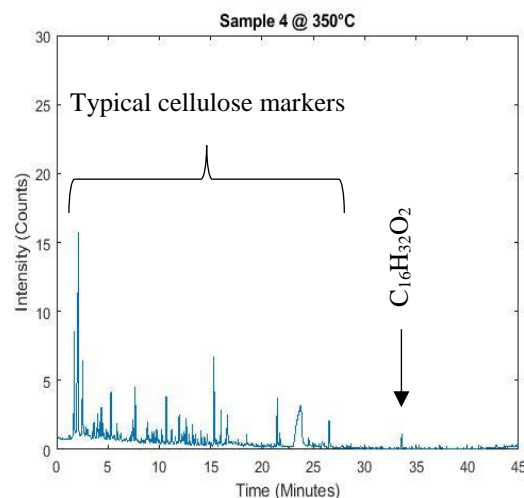


Fig. 4 TIC of field sample 4 from pyrolysis at 350C.

At 400°C and 450°C species present were all at low intensities and no further species could be identified. However, it is possible that the deposits are removed at 250°C and 350°C but they are masked by the abundance of diesel and cellulose-derived species that is also removed from the filter at these temperatures respectively.

### 3.2 Topographical and elemental analysis by SEM

A control filter, Sample 1, shows the structure of the un-pleated cellulose strands in the filter (Fig. 5).

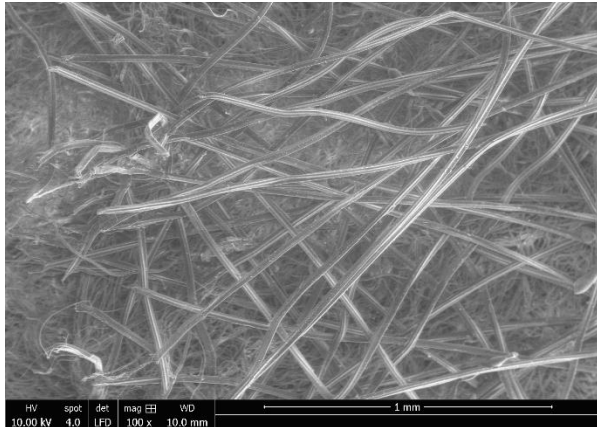


Fig. 5 SEM image of a clean filter, Sample 1.

In comparison, field samples exhibit a variety of different deposits. Field sample 3 appeared to have a film like layer between the cellulose strands (Fig. 6), EDX on the area 1.1 showed C, O and Na (Table 2) suggested by Barker [7] to be a result of the presence of sodium soaps. Trace amounts of S and Si were also detected, which may be accumulation from the fuel or contamination.

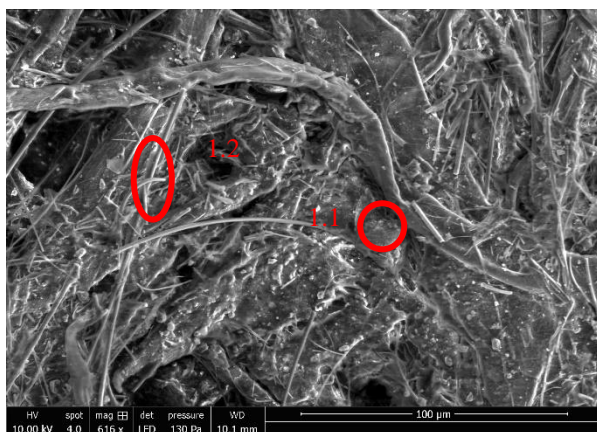


Fig. 6 SEM image of field filter sample 3, with elemental analysis of the highlighted area shown in table.

Area 1.2 was largely dominated by the presence of Si, O and Na (Table 2). It is thought that this is contamination through handling rather than originating from diesel.

No film was present in samples 4 and 5, although field sample 4 had particle like features attached to the filter fibres (Fig. 7). Elemental analysis on area 2.1 suggested the presence of C and O.

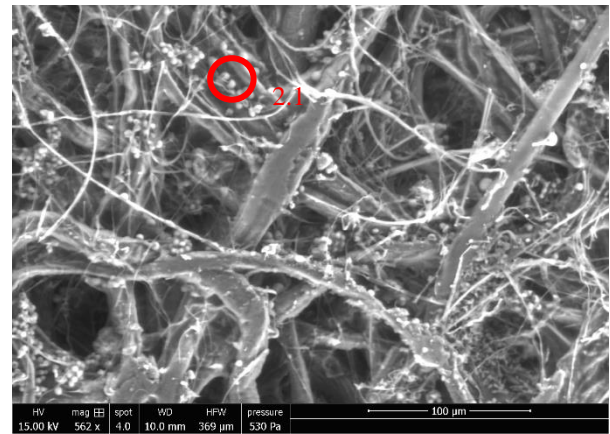


Fig. 7 SEM image of field filter sample 4.

Table 2 Semi-Quantitative elemental analysis of areas on filter samples through EDX.

Element	Abundance (cps eV <sup>-1</sup> )		
	Sample 3, 1.1 (Fig. 6)	Sample 3, 1.2 (Fig. 6)	Sample 4 2.1 (Fig. 7)
<b>C</b>	>30	5	>50
<b>O</b>	10	>40	25
<b>Na</b>	2	20	<1
<b>Si</b>	1	8	1
<b>S</b>	1	<1	<1
<b>Cl</b>	1	<1	<1

Sample 5 had small pieces of debris on the fibres (Fig. 8) though it is not clear whether or not these are as a result of diesel use.

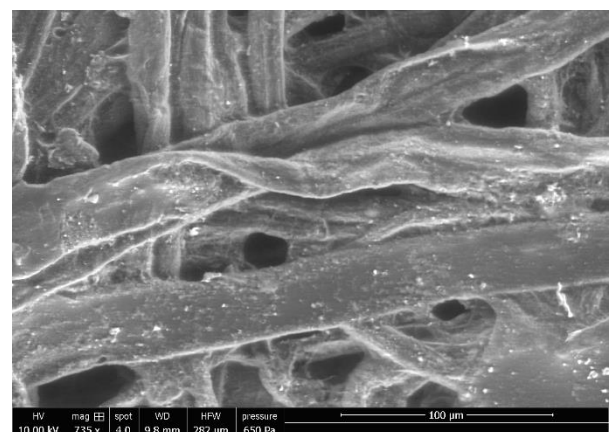


Fig. 8 SEM image of field filter sample 5.

The film seen in field sample 3 was found on the engine test samples 6 and 9. The filtration media of sample 6 was completely covered by a film (Fig. 9), unlike sample 9 (Fig. 10), which was more similar to field sample 3, which had the film between the fibres.

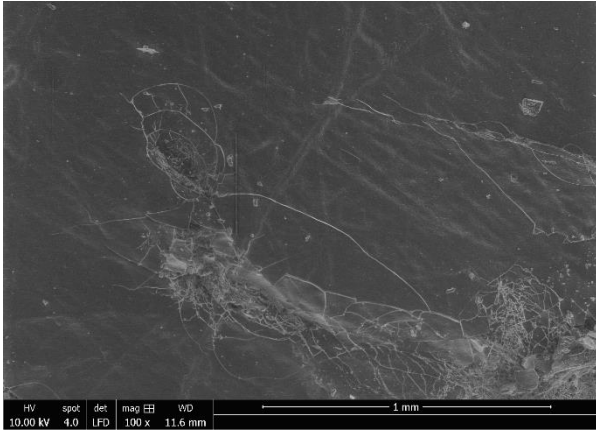


Fig. 9 SEM image of the engine test filter sample 6. Film covers the whole surface of filter.

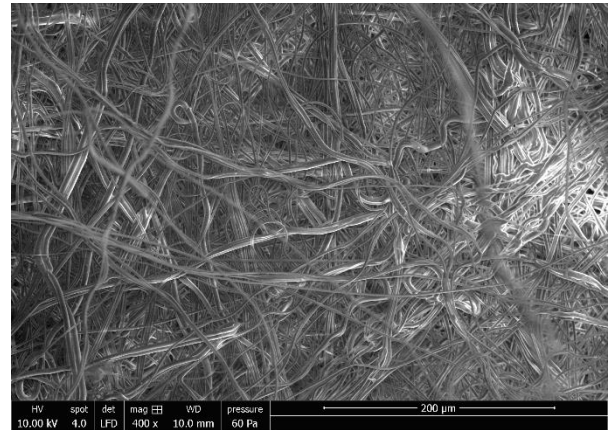


Fig. 11 SEM image of engine test filter sample 8. No film was visible between filter pores.

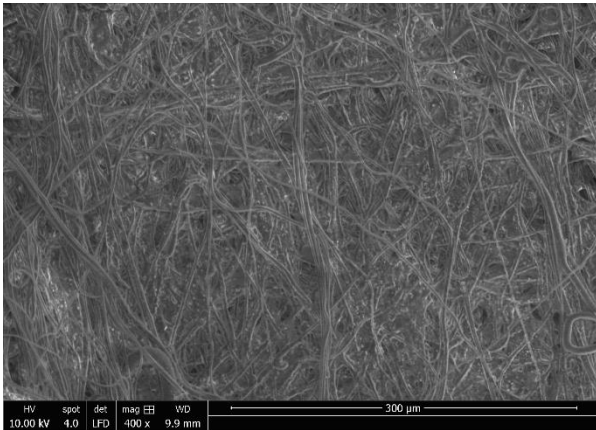


Fig. 10 SEM image of the engine test filter sample 9. Organic film is present in the pores of the filtration media.

The appearance of the organic film in some of the filters is different to the deposit seen on IDIDs [7, 9, 15, 17] which is not surprising as the filter ‘sees’ different operating conditions to the injectors. However, the use of EDX has shown that similar elements are present [8, 9, 14, 21].

Engine test sample 8, which was adulterated with a DCA, sodium and acid species, did not appear to have any deposit present (Fig. 11). Showing the effect of the DCA.

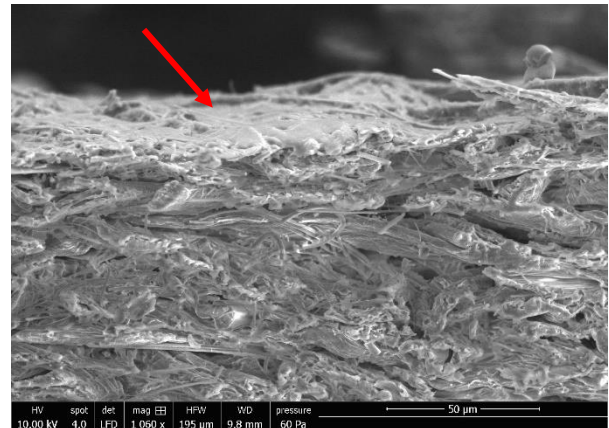


Fig. 12 SEM image of the cross section of filter sample 3.

### 3.3 Chemical analysis of filters by ToF-SIMS

The ToF-SIMS technique can produce both negative and positive ion mass spectra from the surface they are analysing [4]. Analysis of the filter media described in Table 1 showed the following, a number of sodium derived fragment species were present in the positive ion mass spectrum of sample 3 (Fig. 13 A), including sodium-carboxyl groups. The negative spectrum also confirmed the presence of the carboxyl functional group present in the sample (Fig. 13 B).

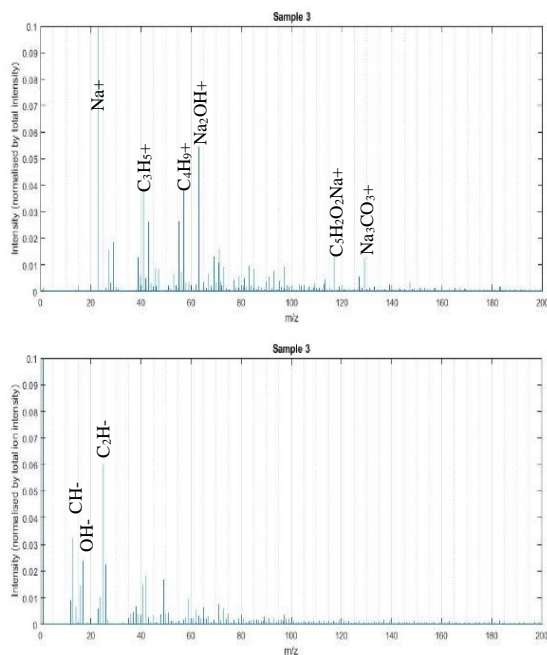


Fig. 13 Positive (A)(Top) and negative (B)(Bottom) ToF-SIMS spectra of field sample 3.

The positive polarity mass spectra of engine filter sample 8 ions is largely dominated by the presence of aliphatic hydrocarbons as well as a monosaccharide ions arising from the cellulose filter (Fig. 14 A). Visual analysis on the SEM of sample 8 did not reveal any film build up (Fig. 11). The functional groups of a carboxylate were not as prevalent in the negative polarity data of sample 8 compared to sample 3 (Fig. 14 B). The reduced presence of sodium and carboxylate compared with field sample 3 suggests the film is a sodium soap, although there is still sodium present.

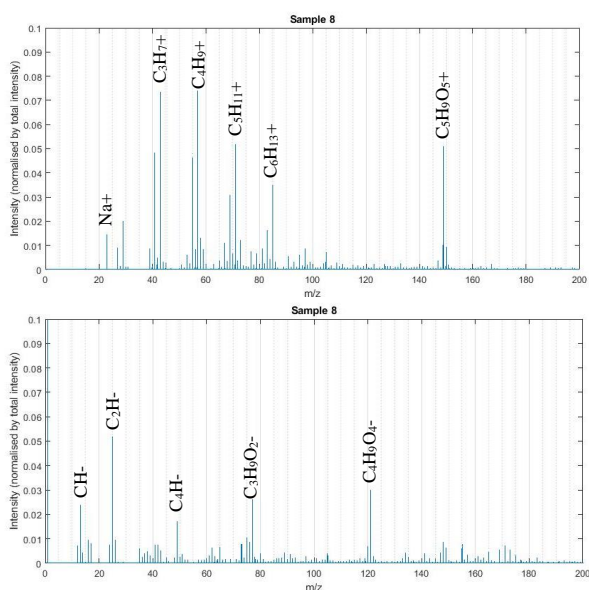


Fig. 14 Positive (A)(Top) and negative (B)(Bottom) ToF-SIMS spectra of engine test sample 8

### 3.4 The application of PCA analysis.

Fig. 15 shows a score plot, for positive polarity ions, of PC1 and PC2 for each sub-sample grouped by its parent sample. Loadings of the principal components indicate what ions for each PC are positively and negatively affected by. Samples were positively displaced along PC1 by the presence of the inorganic sodium, such that samples 3, 6 and 9, which all had an organic film on or in the filter, exhibited greater presence of the ions in comparison to the rest of the samples and thus were displaced to the right of Fig. 15.

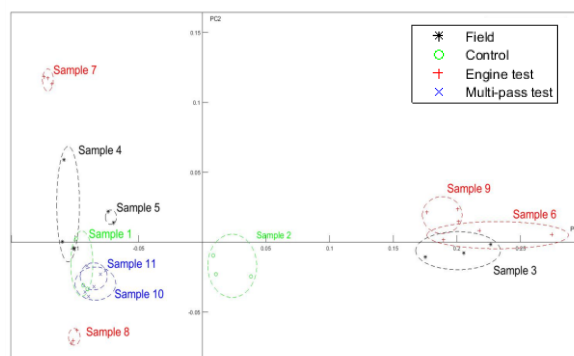


Fig. 15 Scores plot of all filter samples for positive polarity ions. PC1 and PC2 explained 81% and 10% of the variance respectively.

Samples 1, 4, 5, 7, 8, 10, 11 were negatively displaced along PC1. The loadings of PC1 suggested that this is due to the greater presence of aldehyde and ketone ions, likely from the polysaccharides that form the cellulose. This indicates that less deposit is present on the surface of the samples.

High relative amounts of hydroxide ions in the negative polarity ToF-SIMS data of samples 3, 6 and 9, again suggesting the presence of sodium and water species in the film.

Subsample repeats of each sample grouped on the scores plot meaning that the surface chemistry is similar across the samples. Comparison of the sample locations on the scores plot in respect to PC1 and the SEM images indicates that the film seen in Fig. 6, Fig. 9 and Fig. 10 is likely due to the presence of a sodium carboxylate soap reported in previous studies of filter deposits [5-8, 12].

### 4. Conclusion

This initial investigation using the ToF-SIMS technique to determine the nature of deposits on diesel fuel filters successfully confirmed the presence of sodium salts seen by others, and has proven applicable to samples from both research (engine testing, filter rigs) and field samples.

Table 3 Filter references and conclusions.

Filter type	Sample reference	Conclusions
Control	Sample 1	Although a clean filter, presence of sodium inorganic material, but there was no deposit.
Control	Sample 2	No deposit on filter. PCA showed high relative amounts of cellulose markers.
Field USA	Sample 3	Organic film between the cellulose and layered on top of the sample, attributed to the high relative amounts of organic sodium seen from PCA.
Field ASIA	Sample 4	Particle like features attached to the cellulose fibres. No indication as to a difference could have caused this in the first two principal components.
Field EU	Sample 5	Particle like features attached to the cellulose fibres. No indication as to a difference could have caused this in the first two principal components.
Engine test (DW10Bmodified.)	Sample 6	Organic film completely layered on top of the sample, attributed to the high relative amounts of organic sodium seen from PCA.
Engine test (DW10Bmodified.)	Sample 7	No deposit was visible on the filter and low relative amounts of sodium inorganics. High relative amounts of aliphatic hydrocarbon ions, although these were different to those in Sample 8.
Engine test (DW10Bmodified.)	Sample 8	No deposit was visible on the filter and low relative amounts of sodium inorganics. High relative amounts of aliphatic hydrocarbon ions, although these were different to those in Sample 7.
Engine test (DW10Bmodified.)	Sample 9	Organic film between the cellulose of the sample, attributed to the high relative amounts of organic sodium seen from PCA.
Multi-pass test precursor	Sample 10	No deposit on filter. PCA showed high relative amounts of cellulose markers.
Multi-pass test	Sample 11	No deposit on filter. PCA showed high relative amounts of cellulose markers.

The application of PCA to the ToF-SIMS data confirmed that the samples which had a visible continuous film also had contained a high amount of the sodium salt derived species.

Although the PY-GCMSs technique can provide some detail as to the presence of deposits on the filters, the technique is limited because observed fragments are dominated by the removal of diesel and cellulose-derived species.

Topographic images of the filters showed two classes of deposits were present on the filters; films and distinct entities. A cross section of a field filter sample showed that the layer of film was only present on the fuel tank side surface of the filter.

This initial study has shown the applicability of a number of techniques to the characterisation of diesel filter deposits. These and additional techniques will be further explored to understand these deposits and be the subject of further publications.

## References

1. Stanislaus, A., A. Marafi, and M. Rana, *Recent advances in the science and technology of ultra low sulfur diesel (ULSD) production*. Catalysis Today, 2010. **153**(1-2): p. 1-68.
2. Anastopoulos, G., et al., *Impact of oxygen and nitrogen compounds on the lubrication properties of low sulfur diesel fuels*. Energy, 2005. **30**(2-4): p. 415-426.
3. Hazrat, H., M. Rasul, and M. Khan, *Lubricity Improvement of the Ultra-low Sulfur Diesel Fuel with the Biodiesel*. Energy Procedia, 2015. **75**: p. 111-117.
4. Barker, J., et al., *A Novel Technique for Investigating the Nature and Origins of Deposits Formed in High Pressure Fuel Injection Equipment*. SAE Int. J. Fuels Lubr., 2010. **2**(2): p. 38-44.
5. Schwab, S., et al., *Internal Injector Deposits in High-Pressure Common Rail Diesel Engines*. SAE Int. J. Fuels Lubr., 2010. **3**(2): p. 865-878.
6. Lacey, P., et al., *Fuel Quality and Diesel Injector Deposits*. SAE Int. J. Fuels Lubr., 2012. **5**(3): p. 1187-1198.
7. Barker, J., S. Cook, and P. Richards, *Sodium Contamination of Diesel Fuel, its Interaction with Fuel Additives and the Resultant Effects on Filter Plugging and Injector Fouling*. SAE Int. J. Fuels Lubr, 2013. **6**(3): p. 826-838.
8. Trobaugh, C., et al., *Internal Diesel Injector Deposits: Theory and Investigations into Organic and Inorganic Based Deposits*. SAE Int. J. Fuels Lubr., 2013. **6**(3): p. 772-784.

9. Dallanegra, R. and R. Caprotti, *Chemical Composition of Ashless Polymeric Internal Diesel Injector Deposits*. SAE Technical Paper 2014-01-2728, 2014.
10. Feld, H. and N. Oberender, *Characterization of Damaging Biodiesel Deposits and Biodiesel Samples by Infrared Spectroscopy (ATR-FTIR) and Mass Spectrometry (TOF-SIMS)*. SAE J. Fuels Lubr., 2016. **9**(3): p. 717-724.
11. Barker, J., et al., *Spectroscopic Studies of Internal Injector Deposits (IDID) Resulting from the Use of Non-Commercial Low Molecular Weight Polyisobutylenesuccinimide (PIBSI)*. SAE Int. J. Fuels Lubr., 2014. **7**(3): p. 762-770.
12. Csontos, B., et al., *Contaminants Affecting the Formation of Soft Particles in Bio-Based Diesel Fuels during Degradation*. SAE Technical Paper 2019-01-0016, 2019.
13. Camerlynck, S. and J. Chandler, *FAME Filterability: Understanding and Solutions*. SAE Int. J. Fuels Lubr., 2012. **5**(3): p. 968-976.
14. Barker, J., et al., *The Characterisation of Diesel Internal Injector Deposits by Focused Ion-Beam Scanning Electron Microscopy (FIB-SEM), Transmission Electron Microscopy (TEM), Atomic Force Microscopy and Raman Spectroscopy*. SAE Technical Paper 2015-01-1826, 2015.
15. Chaikool, P., K. Intravised, and P. Patsin, *A Study of Effect of Biodiesel on Common-Rail Injection Nozzle*. SAE Int. J. Fuels Lubr., 2016. **9**(3): p. 712-716.
16. Smith, A. and R. Williams, *Linking the Physical Manifestation and Performance Effects of Injector Nozzle Deposits in Modern Diesel Engines*. SAE Int. J. Fuels Lubr., 2015. **8**(2): p. 344-357.
17. Barker, J., et al., *The Application of New Approaches to the Analysis of Deposits from the Jet Fuel Thermal Oxidation Tester (JFTOT)*. SAE Int. J. Fuels Lubr., 2017. **10**(3): p. 143.
18. Barker, J., C. Snape, and D. Scurr, *Information on the Aromatic Structure of Internal Diesel Injector Deposits From Time of Flight Secondary Ion Mass Spectrometry (ToF-SIMS)*. SAE Technical Paper 2014-01-1387, 2014.
19. Trindade, G., M.-L. Abel, and J. Watts, *simsMVA: A tool for multivariate analysis of ToF-SIMS datasets*. Chemometrics and Intelligent Laboratory Systems, 2018. **182**: p. 180-187.
20. Riedo, C., D. Scalaronea, and O. Chiantore, *Multivariate analysis of pyrolysis-GC/MS data for identification of polysaccharide binding media*. Analytical Methods, 2013. **5**: p. 4060-4067.
21. Fortunato, M., et al., *Are Internal Diesel Injector Deposits (IDID) Mainly Linked to Biofuel Chemical Composition or/and Engine Operation Condition?* SAE Technical Paper 2019-01-0061, 2019.